

Geophysical Research Letters[®]



RESEARCH LETTER

10.1029/2023GL106076

Key Points:

- Horizontal radiative transfer (RT) enhances cloud-top longwave radiative cooling across the stratocumulus-to-cumulus transition regime
- Cloud-top cooling enhancement due to horizontal RT maximizes in the middle stage of the stratocumulus-to-cumulus transition
- Sharp radiative heating gradient throughout the cloud layer cannot be resolved with a coarse model vertical resolution

Supporting Information:

Supporting Information may be found in the online version of this article.

Correspondence to:

T. Ren,
tr7585@tamu.edu

Citation:

Ren, T., Yang, P., Huang, X., Chen, X., & Shen, Z. (2023). Enhanced cloud top longwave radiative cooling due to the effect of horizontal radiative transfer in the stratocumulus to trade cumulus transition regime. *Geophysical Research Letters*, 50, e2023GL106076. <https://doi.org/10.1029/2023GL106076>

Received 24 AUG 2023

Accepted 8 NOV 2023

Enhanced Cloud Top Longwave Radiative Cooling Due To the Effect of Horizontal Radiative Transfer in the Stratocumulus to Trade Cumulus Transition Regime

Tong Ren¹ , Ping Yang¹ , Xianglei Huang² , Xiuhong Chen² , and Zhaoyi Shen³ 

¹Department of Atmospheric Sciences, Texas A&M University, College Station, TX, USA, ²Department of Climate and Space Sciences and Engineering, University of Michigan, Ann Arbor, MI, USA, ³Department of Environmental Science and Engineering, California Institute of Technology, Pasadena, CA, USA

Abstract Recent studies develop the SPeedy Algorithm for Radiative TrAnSfer through CloUd Sides (SPARTACUS) to handle the influence of horizontal RT on vertical radiative fluxes within an atmospheric column. The present study applies SPARTACUS to large eddy simulation (LES)-generated cloud fields across the stratocumulus to trade cumulus transition (STCT) regime with coarse and fine vertical resolutions. The results show that, as the vertical resolution increases, radiation simulations show increasingly stronger cloud-top longwave (LW) radiative cooling. Consequently, the sharp radiative heating gradient across the cloud layer in the LES-like resolution simulations cannot be resolved with the coarse resolution simulations. Including the horizontal RT typically enhances cloud LW radiative cooling rate by less than 10% for all the cloud fields but more significantly in the cloud fields during the STCT. The enhanced cloud LW radiative cooling also occurs in the lower cloud layer in the decoupled cumulus cloud regime.

Plain Language Summary In conventional climate studies, the intricate interplay of light within clouds, particularly from the sides, is often overlooked. Recent advancements have introduced a more efficient method for accounting for lateral light transfer in cloud modeling. This study employs this novel approach to examine how different configurations of low-level clouds, generated by computer models, influence atmospheric heating. Our findings demonstrate that providing finer details of cloud structures leads to a cooling effect at the uppermost regions of the clouds. This emphasizes the importance of representing clouds in high resolution for accurate climate assessments. Moreover, when lateral light transfer is considered, the cooling effect intensifies across various cloud patterns. This phenomenon is most pronounced during the transition from uniform dispersion to a more scattered distribution of clouds. Additionally, we observed this cooling effect in the lower cloud layer when clouds are in a scattered formation.

1. Introduction

Radiative transfer (RT) schemes in current General Circulation Models (GCMs) do not consider horizontal photon transport for computational efficiency. However, neglecting horizontal RT through cloud sides leads to errors in computed radiative fluxes when the ratio of cloud vertical extent to horizontal extent increases in a model grid box (Gu & Liou, 2001), which is happening now as the GCM horizontal and vertical resolutions have become increasingly higher. Based on large eddy simulation (LES)-generated distributions of three distinct tropical cloud types, Singer et al. (2021) assessed the shortwave (SW) radiative flux and cloud albedo biases resulting from the omission of horizontal RT and approximated an annual-mean 1D RT scheme computed radiative flux bias of $3.1 \pm 1.6 \text{ W m}^{-2}$ at the top of the atmosphere across tropical regions. Efforts have been made by researchers to create computationally efficient RT solvers that consider horizontal RT. Jakub and Mayer (2015) expanded upon the 1D two-stream method (Meador & Weaver, 1980) to develop the TenStream solver, which incorporates 10 streams to account for radiative transfers between vertically and horizontally adjacent model grid boxes. To utilize the TenStream solver, it is necessary to pre-calculate and store the exchange coefficients associated with the streams, based on the grid box size and the bulk absorption and scattering properties of the media in each grid box within the computational domain (Jakub & Mayer, 2015). In a similar manner, Hogan and Shonk (2013) integrated the impact of horizontal RT on vertical radiative fluxes in a grid box by using linear terms in the two-stream equations to represent radiative energy exchanges between clear-sky and cloudy areas. This approach was later named the SPeedy Algorithm for Radiative TrAnSfer through CloUd Sides (SPARTACUS) after being

© 2023. The Authors.

This is an open access article under the terms of the [Creative Commons Attribution-NonCommercial-NoDerivs License](https://creativecommons.org/licenses/by-nc-nd/4.0/), which permits use and distribution in any medium, provided the original work is properly cited, the use is non-commercial and no modifications or adaptations are made.

refined and expanded to include the longwave (LW) spectrum (Hogan et al., 2016; Schäfer et al., 2016). Additionally, clouds at a higher altitude have the ability to trap upward solar radiation that is reflected by lower-level objects not underneath the higher-altitude clouds. Hogan et al. (2019) further incorporated this entrapment effect into the SPARTACUS solver, which is available as an option in the European Center for Medium-Range Weather Forecasts (ECMWF) radiation scheme *ecRad* (Hogan & Bozzo, 2018). While TenStream is for resolved 3D effects in high resolution models, SPARTACUS is for unresolved 3D effects in low resolution models. In other words, TenStream deals with horizontal RT between model grid boxes (i.e., inter-column light transport), and SPARTACUS deals with horizontal RT within every model grid box (i.e., sub-grid light horizontal transport). Hence, TenStream and SPARTACUS are often used in different contexts for different purposes.

Despite the consideration of the impact of horizontal RT on vertical radiative fluxes, at present, the computational speed of the SPARTACUS solver is six-fold slower than that of the widely used Monte Carlo Independent Column Approximation (McICA; Pincus et al., 2003) solver in climate models (Hogan & Bozzo, 2018; Ren et al., 2022). Nevertheless, computationally intensive schemes are frequently employed by the climate modeling community for specific applications. For instance, the Multiscale Modeling Framework (MMF; Grabowski, 2001; Khairoutdinov & Randall, 2001) and the Framework for Improvement by Vertical Enhancement (FIVE; Yamaguchi et al., 2017) were developed to enhance cloud representations in climate models. Therefore, the SPARTACUS solver may be employed in climate simulations when horizontal RT plays a crucial role in the problem of interest.

The 3D RT solvers outperform 1D RT solvers in calculating the proportions of direct and diffusive solar radiation reaching the surface, which are important to the employment of solar energy systems (Villefranque & Hogan, 2021). Compared to 1D RT solvers, applying 3D RT solvers to detailed cloud fields produce more realistic surface solar irradiance spatial distributions, which in turn influence surface turbulent heat flux and cloud spatial distributions (Jakub & Mayer, 2017; Veerman et al., 2020, 2022). Cloud top LW radiative cooling plays an important role in maintaining a stratocumulus-topped marine boundary layer by compensating for the warming caused by the air entrained from above (Lilly, 1968). Due to the influence of horizontal RT on cloud top LW radiative cooling and associated cloud microphysics and dynamics (Klinger et al., 2017, 2019), the SPARTACUS solver may be adopted to study the stratocumulus to trade cumulus transition (STCT). Hence, it would be helpful to know the difference in computed radiative heating rates between the SPARTACUS solver and the 1D solver for the cloud regimes throughout the STCT. This study performs offline SPARTACUS and 1D LW radiation simulations for seven LES-generated cloud field snapshots across the STCT track over northeastern Pacific. The simulation results of SPARTACUS are compared with those of TripleClouds, the equivalent solver without 3D effects (Shonk & Hogan, 2008). The data and methods are introduced in Section 2, followed by the simulation results in Section 3. The conclusions are drawn in Section 4.

2. Model, Data, and Methods

This study uses three different solvers in *ecRad*, independent column approximation (ICA) two-stream homogeneous, TripleClouds, and SPARTACUS. Tripleclouds solver that approximates the cloud water mass variation at a given height by one optically thick cloud region and one optically thin cloud region (Shonk & Hogan, 2008). If the Tripleclouds cloud structure description is used in the SPARTACUS solver, then the difference between Tripleclouds and SPARTACUS simulations with identical inputs is just the cloud 3D effect. The SPARTACUS simulations in this study are all based on the Tripleclouds cloud structure description. Compared to conventional RT solvers, such as the two-stream homogeneous solver, one more input parameter, the cloud water content fractional standard deviation (f_{σ}) is required to run the Tripleclouds solver; two more input parameters, f_{σ} and the normalized cloud perimeter length (L_c) in each cloud layer, are required to run the SPARTACUS solver. To quantify f_{σ} , the ratio of the standard deviation of in-cloud water content to the mean in-cloud water content, the cloud water content sub-grid variability needs to be provided. The sub-grid variability of cloud water content may be assumed or diagnosed (e.g., Ahlgrimm & Forbes, 2017). Some GCMs (e.g., Bogenschutz et al., 2012) have adopted the probability density function (PDF)-based boundary layer cloud parameterization scheme (Golaz et al., 2002) to treat shallow convection. This kind of PDF-based scheme achieves the turbulence closure through a joint PDF of vertical velocity, temperature, and moisture, based on which f_{σ} can be derived. If the PDF-based scheme is also adapted to deep convection, then f_{σ} can be derived for all clouds. The other input parameter L_c is often estimated in terms of cloud faction (f_c) and cloud size (Hogan et al., 2019). A parameterization of L_c in terms of the model horizontal grid spacing has been proposed (Fielding et al., 2020). In addition, the SPARTACUS

solver is built upon the exponential-random cloud overlapping treatment (Hogan & Illingworth, 2000), which is different from the random and maximum-random cloud overlapping assumptions made in conventional RT solvers. Methods of linking the cloud overlap parameter (α) or the decorrelation length in the exponential-random cloud overlapping treatment to prognostic variables in GCMs have been suggested (Jing et al., 2016, 2018; Lebrun et al., 2023). Using four LES-generated cumulus cases, Villefranque et al. (2021) calibrated f_c , L_c , and α against 3D Monte Carlo RT simulations.

In this study, parameters f_c and α were derived from the LES-generated cloud fields described in Shen et al. (2022), which developed a public cloud field library for GCM parameterization calibrations with a focus on the STCT process over the east Pacific using the Python Cloud LES (PyCLES; Pressel et al., 2015). They selected a few sites along two STCT tracks in the northeastern and southeastern Pacific, respectively. The historical simulations from the Coupled Model Intercomparison Project Phase 5 (CMIP5; Taylor et al., 2012) archive, specifically the HadGEM2-A and CNRM-CM5 atmosphere-only simulations, were used to drive the PyCLES with the approach described in Shen et al. (2020). Each PyCLES experiment integrated the model for 6 days, and the resulting simulated 3D cloud field data at the end of this time period were saved. We used the 3D cloud distributions from the LES runs at the seven sites along the northeastern Pacific STCT track forced by the CNRM-CM5 large-scale averages in July during the years 2004–2008, as these simulations exhibited the smoothest STCT based on the results presented by Shen et al. (2022). The locations of the selected 7 sites from northeast to southwest are Site 17 (34.32°N, 125.28°W), Site 18 (31.52°N, 129.60°W), Site 19 (28.72°N, 133.59°W), Site 20 (25.91°N, 136.41°W), Site 21 (23.11°N, 140.63°W), Site 22 (20.31°N, 144.84°W), and Site 23 (17.51°N, 149.06°W), respectively. Figure 1 shows the column-integrated liquid water path (LWP) distributions and associated cloud fraction (f_c) profiles of the selected LES-generated STCT regime. The domain of the LES runs is 6 km wide and 4 km tall. The horizontal and vertical grid spacings are 75 and 20 m, respectively.

Current GCMs have vertical resolutions of around 200 m in the lower troposphere (Bogenschutz et al., 2021). Bogenschutz et al. (2021) showed that increasing the vertical resolution between 995 and 700 hPa to a LES-like one (about 10 m) in the Department of Energy's Energy Exascale Earth System Model version 1 (E3SMv1; Golaz et al., 2019) significantly reduces the negative bias of the marine low-level cloud amount in this model. The distinct second and third vertical velocity moments produced in the LES-like simulation resemble the theoretical stratocumulus-topped marine boundary layer most and hence primarily account for the improved marine low-level cloud representation (Bogenschutz et al., 2021). Lee et al. (2021) implemented FIVE into the E3SM and found a significant increase of marine low-level cloud amount at the LES-like vertical resolution using the E3SM-FIVE. Due to the trend of increasing model vertical resolution for better resolved low-level clouds in the GCM community, we perform offline radiation simulations using the LES-generated cloud fields at the original 20 m vertical resolution and the cloud fields coarsened to 40, 100, and 200 m vertical resolutions, respectively, below 2 km to show the vertical resolution influence on radiation simulations. The coarsened cloud profile is obtained by averaging liquid cloud mass mixing ratios in 20 m vertical resolution grid boxes within each coarser grid box. Figure S1 in Supporting Information S1 shows cloud fraction profiles at the four vertical resolutions below 2 km. From Site 17 to Site 23, cloud top layer is gradually elevated and associated cloud fraction gradually reduces, characteristics of a STCT.

With the LES-generated and subsequently coarsened cloud fields, the *ecRad* 1.4.0 is used to perform ICA, Tripleclouds, and SPARTACUS (3D) radiation simulations. In the ICA simulations, the two-stream homogeneous solver is selected to compute radiative fluxes for every column within the 6×6 km² domain; subsequently, computed radiative fluxes are averaged over the domain to calculate the domain-averaged radiative heating rate. In the Tripleclouds and 3D simulations, the domain-averaged radiative fluxes are calculated directly with the Tripleclouds and SPARTACUS solvers and cloud statistics within the whole domain. Temperature and specific humidity profiles below 2 km and above 5 km are taken from the domain-averaged LES data and forcing data, respectively. To guarantee smooth temperature and humid variations between 2 and 5 km, temperature and specific humidity profiles between 2 and 5 km are obtained via interpolations. Ozone profiles are obtained by averaging the version 5 of the ECMWF atmospheric reanalysis (ERA5) monthly averaged data (Hersbach et al., 2023) in July during 2004–2008. As in previous studies (e.g., Ren et al., 2020), the volume mixing ratios of CO₂, CH₄, and N₂O are set to the values of 390.5, 1.803, and 0.3242 ppmv, respectively, same as in the Fifth Assessment Report of the Intergovernmental Panel on Climate Change. The bottom and top of the atmosphere are set to 0 and 30 km, respectively. Vertical resolutions are fixed to 1 km between 2 and 25 and 2.5 km between

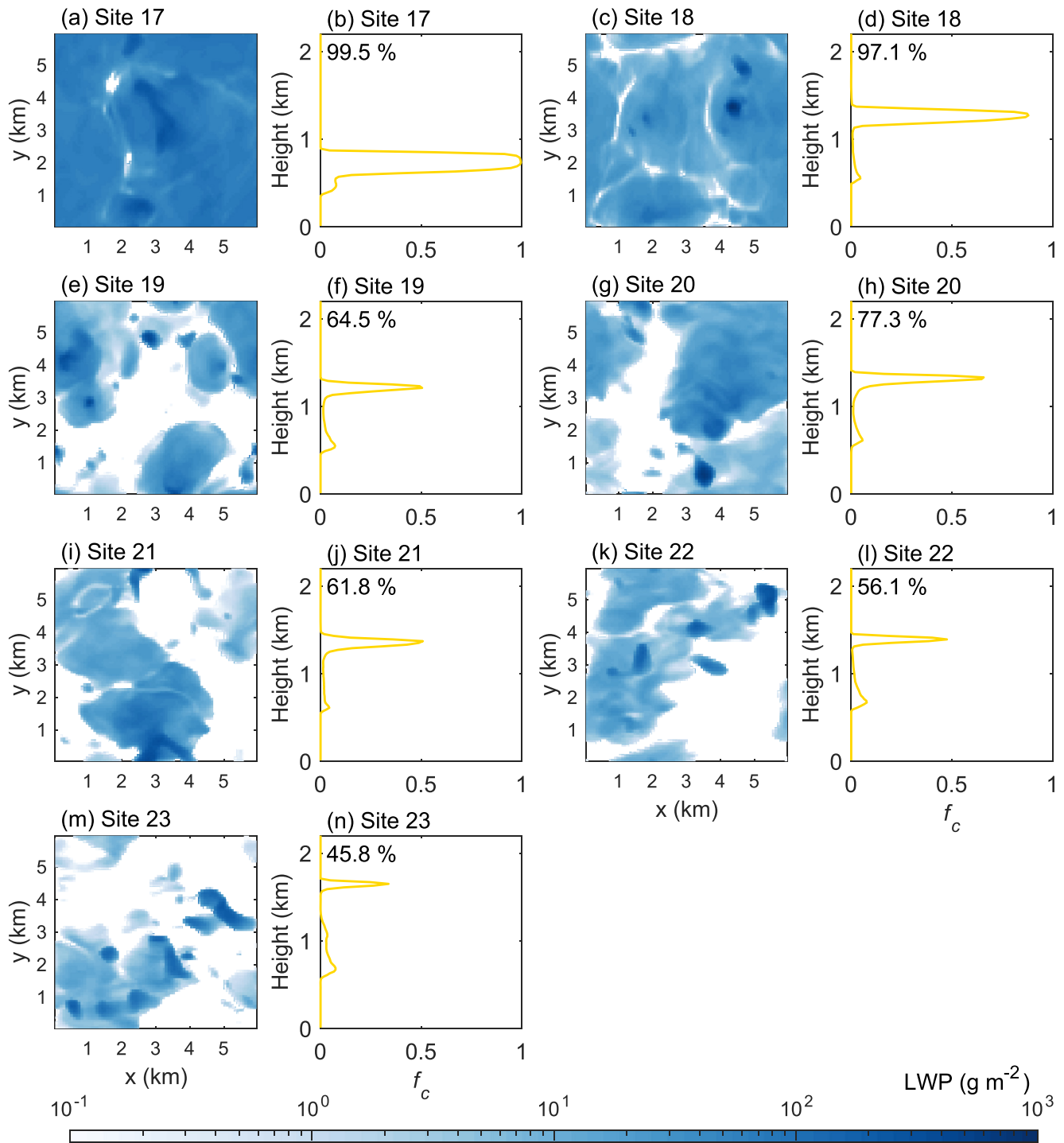


Figure 1. The column-integrated liquid water path (LWP; g m^{-2}) distributions of the simulated cloud fields at the end of the 6-day time integration from the LES experiment forced by the CNRM-CM5 large-scale averages in July during 2004–2008 ((a), (c), (e), (g), (i), (k), and (m)) and associated cloud fraction (f_c) profiles at the 20 m original vertical resolution ((b), (d), (f), (h), (j), (l), and (n)) across the seven sites over the northeastern Pacific in Shen et al. (2022). The number in each f_c plot is the total cloud cover.

25 and 30 km. Surface emissivity is assumed to be unity across the LW spectrum. Surface skin temperature is set to the temperature at the bottom of the atmosphere.

We add the Moderate Resolution Imaging Spectroradiometer (MODIS) Collection 6 (MC6) liquid cloud optical property model (Platnick et al., 2017) to the *ecRad* 1.4.0 for the radiation simulations. The bulk optical properties

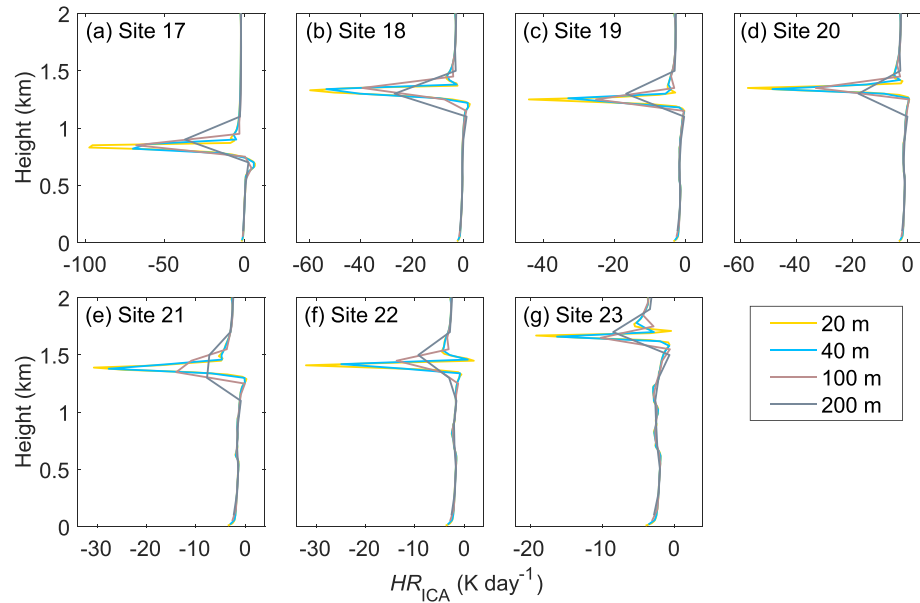


Figure 2. Domain-averaged broadband LW radiative heating rate (K day^{-1}) profiles simulated by the *ecRad* ICA (HR_{ICA}) with vertical resolutions of 20, 40, 100, and 200 m, respectively, below 2 km at the selected seven sites over the northeastern Pacific.

of the MC6 liquid cloud model are almost the same as those of the SOCRATES liquid cloud model in *ecRad* 1.4.0 in the LW except that the single-scattering albedo of the MC6 model is smaller than that of the SOCRATES model in the $2,600\text{--}3,250\text{ cm}^{-1}$ band (not shown). In the *ecRad* simulations, the effective radius is fixed to $10\ \mu\text{m}$ for simplicity, as in previous studies (e.g., Marshak et al., 2006). In the 3D simulations, f_{σ} in each cloud layer is derived from the LES-generated cloud water content distribution; α between two adjacent cloud layers is derived from the LES-generated cloud fractions of the two layers (Hogan & Illingworth, 2000). If the total cloud cover of two adjacent cloud layers exceeds what would be expected with random overlap, it is assumed that the two cloud layers overlap randomly by assigning an α of zero. The 3D simulations consist of two sets of SPARTACUS simulations with the L_c parameterization schemes of Fielding et al. (2020) and Ren et al. (2022), respectively. We also perform the ICA radiation simulations using the more accurate 16-stream Discrete Ordinate Radiative Transfer (DISORT; Stamnes et al., 1988) solver in the LW version of the Rapid RT Model (Mlawer et al., 1997). The RRTM simulated radiative heating rate profiles are used to evaluate those simulated by the *ecRad* ICA.

3. Results

The *ecRad* ICA simulated domain-averaged LW radiative heating rate (HR_{ICA}) profiles below 2 km are shown in Figure 2. Simulated cloud top radiative cooling maximizes at where f_c maximizes (Figure S1 in Supporting Information S1 and Figure 2). The domain-averaged radiative cooling in the cloud layer weakens from Site 17 to Site 23 in general (Figure 2), except that Site 19 breaks the monotony. As shown in Figure 1 and Figure S1 in Supporting Information S1, f_c generally decreases from the coastal region (Site 17) to the region farthest way from the continent (Site 23) except that f_c is smaller at Site 19 than at Site 20. As the vertical resolution increases from 200 to 20 m, the cloud layer cooling peak becomes progressively stronger (Figure 2). At the Site 17, the HR_{ICA} minimum decreases from $-37.4\ \text{K day}^{-1}$ at the 200 m resolution to $-97.7\ \text{K day}^{-1}$ at the 20 m resolution. In other words, the sharp vertical gradient of LW radiative heating rate across the cloud layer cannot be simulated with the coarse vertical resolution in current models. It is well known that the spike in LW cooling at the top of stratocumulus is only around 50 m thick (e.g., Ackerman et al., 1995), so it is not a surprise to learn that if the vertical resolution is too coarse, the peak will be underestimated and smeared out. Bellon and Geoffroy (2016) suggested that an adequately fine representation of cloud top LW radiative cooling is necessary to produce vigorous downward mixing, an important source of the turbulent kinetic energy that sustains the stratocumulus-topped boundary layer. Hence, the better resolved sharp in-cloud vertical radiative heating rate gradient at the 20 m resolution shown in Figure 2 may contribute to explaining why increasing model vertical resolution to a LES-like

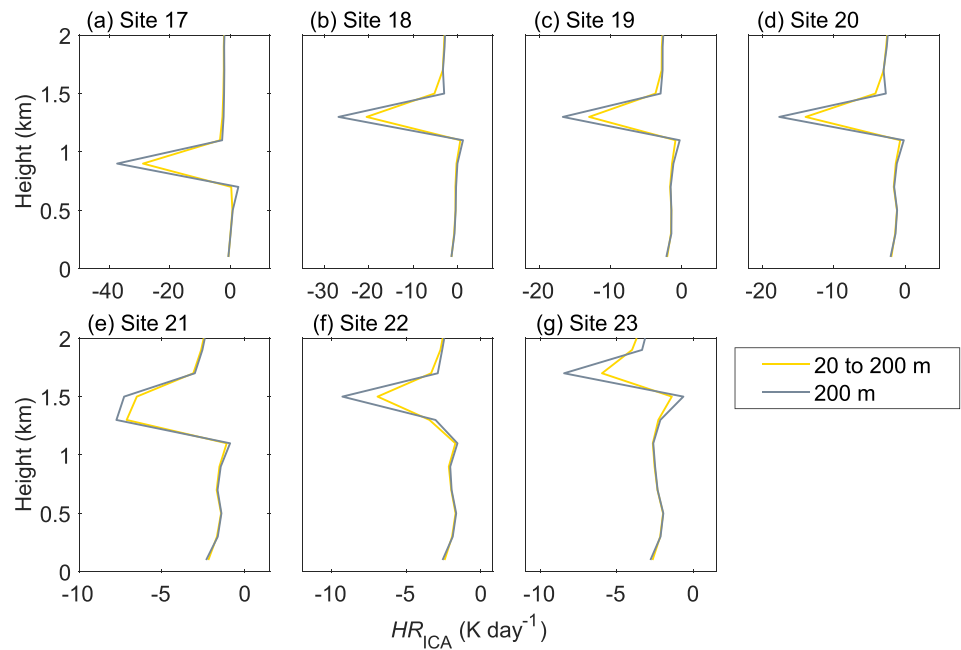


Figure 3. The *ecRad* ICA simulated broadband LW radiative heating rate (HR_{ICA} ; $K day^{-1}$) profiles at the 200 m vertical resolution below 2 km at the selected seven sites over the northeastern Pacific. In each panel, the yellow curve is the simulated 20 m HR_{ICA} averaged to the 200 m vertical resolution; the gray curve is the simulated 200 m HR_{ICA} .

one can significantly increase the E3SM simulated marine low-level cloud amount (Bogenschutz et al., 2021; Lee et al., 2021). Figure S2 in Supporting Information S1 is same as Figure 2 except that the difference between domain-averaged and clear-sky heating rates (i.e., the cloud radiative effect; $HR_{ICA} - HR_{ICA,clr}$) is shown.

As evidenced by the LW radiation flux divergence (Table S1 in Supporting Information S1), the full LW radiative cooling in the lowest 2 km atmosphere is less strong in the 20 m resolution simulations than in the 200 m resolution simulations across the seven sites. Because radiative cooling rate in the LW is dependent upon not only absorption and scattering but also emission, the computed LW radiative difference between different resolutions may be due to the resolution dependence of computed cloud and clear-sky emissions as a consequence of temperature vertical variation. If the HR_{ICA} computed with the 20 m resolution cloud fields is coarsened to the 200 m resolution, the cloud top LW radiative cooling peak is less strong and “wings” above and below are stronger than that directly computed with the 200 m resolution cloud fields obtained through a coarsening of the 20 m resolution cloud fields (Figure 3). Figure S3 in Supporting Information S1 is same as Figure 3 except that HR_{ICA} is replaced with $HR_{ICA} - HR_{ICA,clr}$. The *ecRad* ICA simulated HR_{ICA} profiles are generally close to those simulated by the RRTM ICA above and below the cloud layer, except that the differences can be greater than $0.5 K day^{-1}$ in the lowest 200 m at the 20 m vertical resolution (Figure S4 in Supporting Information S1). In the cloud layer, *ecRad* ICA simulated cooling is stronger than that simulated by the RRTM ICA (Figure S4 in Supporting Information S1) and the magnitude of the difference is comparable to that caused by cloud 3D effect (shown below).

Horizontal RT leads to enhanced cloud top LW radiative cooling throughout the STCT regime (Figure 4). The enhanced cloud cooling is strongest at Sites 19–21 (Figure 4), where the cloud fields are in the middle stage of the STCT and have around 0.5 cloud fractions in the cloud top layers (Figure 2). Hogan et al. (2016) also reported enhanced cloud top LW radiative cooling due to horizontal RT for a cumulus cloud case, to which published broadband LW evaluation of SPARTACUS against Monte Carlo calculations is limited. Kablick et al. (2011) compared backward 3D Monte Carlo and ICA broadband LW heating rates for six LES-generated cloud scenes. They showed that while the 3D effect enhances the cloud top cooling via the mechanism described in Figure 1c of Hogan and Shonk (2013), neglecting the 3D effect introduces an around 2% mean error and a $2.17 K day^{-1}$ maximum difference to computed heating rates from the domain-averaged perspective. In addition, it appears that the simulated cloud top cooling due to the 3D effect is increasingly stronger as the vertical resolution decreases

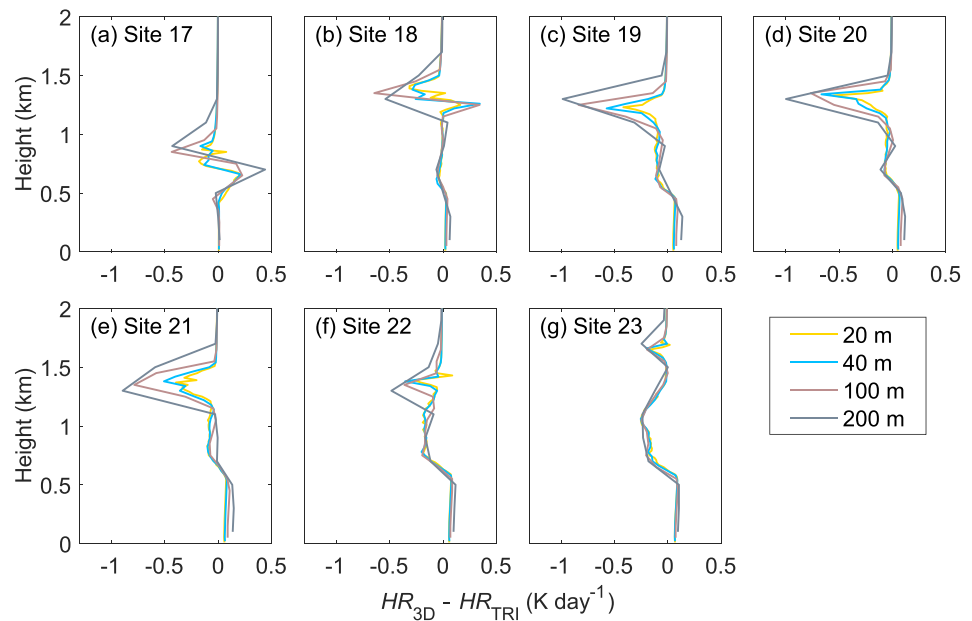


Figure 4. Differences (3D effect) in domain-averaged broadband LW radiative heating rate (K day^{-1}) profiles between the *ecRad* Tripleclouds (HR_{TRI}) and 3D (HR_{3D}) simulations with vertical resolutions of 20, 40, 100, and 200 m, respectively, below 2 km at the selected seven sites over the northeastern Pacific. In the 3D simulations, L_c is parameterized as in Fielding et al. (2020).

(Figure 4). The cloud top cooling enhancement in the 200 m resolution simulations reaches 5.8% at Site 19, 5.9% at Site 20%, and 12.2% at Site 21. The cooling enhancement is less than 1.1% at Site 17, 2.1% at Site 18, 1.4% at Site 22%, and 2.9% at Site 23 regardless of the vertical resolution. In the trade cumulus regime at Sites 22 and 23, the weak cooling enhancement also occurs in the around 0.6 km lower cloud layer whose cloud fraction is slightly greater than those at other sites (Figure S1 in Supporting Information S1 and Figure 4). If the L_c is parameterized as in Ren et al. (2022), the SPARTACUS simulated LW radiative heating rate (HR_{SPA}) profiles are close to those with the L_c parameterization of Fielding et al. (2020) (Figure 4 and Figure S5 in Supporting Information S1). The computed cloud top cooling with the L_c parameterization of Ren et al. (2022) is slightly stronger than that with the L_c parameterization of Fielding et al. (2020) at Site 17 and slightly weaker than those with the L_c parameterization of Fielding et al. (2020) at the rest of the seven sites. While the L_c parameterization of Ren et al. (2022) assumes that clouds tend to aggregate, the L_c parameterization in Fielding et al. (2020) is developed based on a wide range of observed and simulated cloud fields. Consequently, the parameterized L_c and simulated cloud 3D effect are slightly smaller in Ren et al. (2022) than in Fielding et al. (2020) except for the near overcast situation, such as the situation at Site 17. Figure S6 in Supporting Information S1 is same as Figure 4 except that the difference between *ecRad* ICA (HR_{ICA}) and 3D (HR_{3D}) simulations is shown. Figure S7 is same as Figure S6 in Supporting Information S1 except that L_c is parameterized as in Ren et al. (2022).

4. Summary and Conclusions

As a fast 3D RT solver, the recently developed SPARTACUS solver has the potential of being applied to climate simulations, particularly for studying the problems where horizontal RT is important. It has long been known that cloud top LW radiative cooling plays an important role in sustaining the stratocumulus-topped marine boundary layer. In this study, with the LES-generated cloud fields throughout the STCT as input, we performed offline *ecRad* ICA, Tripleclouds, and SPARTACUS radiation simulations to quantify the impact of horizontal RT on the simulated cloud top LW radiative cooling. The simulation results are dependent on the vertical resolution. The simulated sharp radiative gradient across the cloud layer at the LES-like vertical resolution cannot be resolved with a coarse vertical resolution in current GCMs. The result is supportive of the efforts made to resolve the sharp radiative gradient, such as the local vertical resolution enhancement (Yamaguchi et al., 2017) and including the radiation scheme in FIVE (Lee et al., 2021). Horizontal RT enhances cloud top LW radiative cooling throughout

the STCT but the enhancement maximizes in the intermediate stage of the STCT. In addition, cloud top SW radiative heating affects the diurnal cycle of low-level cloudiness (Wyant et al., 1997). How horizontal RT influences the cloud top SW radiative heating across the STCT will be studied in the future. Given the same large-scale subsidence and sea surface temperature distributions, enhanced cloud top LW radiative cooling is favorable for maintaining a well-mixed stratocumulus-topped marine boundary layer. Based on the offline radiation simulation results in this study, we expect that including horizontal RT in GCMs would slow down the stratocumulus breakup and hence shift the subtropical marine stratocumulus breakup region westward.

Data Availability Statement

The offline ECMWF radiation scheme (*ecRad*) 1.4.0 is preserved by Hogan (2020). The LW version of RRTM (RRTM_LW) is preserved by Atmospheric and Environmental Research (2010). The LES cloud field and associated forcing data are available at Ren (2023). The ERA5 monthly averaged ozone data at pressure levels are available at Hersbach et al. (2023).

References

- Ackerman, A. S., Hobbs, P. V., & Toon, O. B. (1995). A model for particle microphysics, turbulent mixing, and radiative transfer in the stratocumulus-topped marine boundary layer and comparisons with measurements. *Journal of the Atmospheric Sciences*, 52(8), 1204–1236. [https://doi.org/10.1175/1520-0469\(1995\)052<1204:AMFPMT>2.0.CO;2](https://doi.org/10.1175/1520-0469(1995)052<1204:AMFPMT>2.0.CO;2)
- Ahlgrimm, M., & Forbes, R. M. (2017). Regime dependence of ice cloud heterogeneity—A convective life-cycle effect? *Quarterly Journal of the Royal Meteorological Society*, 143(709), 3259–3268. <https://doi.org/10.1002/qj.3178>
- Atmospheric and Environmental Research. (2010). RRTM_LW (version 3.3) [Software]. RTWEB. Retrieved from http://rtweb.aer.com/rtrtm_frame.html
- Bellon, G., & Geoffroy, O. (2016). How finely do we need to represent the stratocumulus radiative effect? *Quarterly Journal of the Royal Meteorological Society*, 142(699), 2347–2358. <https://doi.org/10.1002/qj.2828>
- Bogenschutz, P. A., Gettelman, A., Morrison, H., Larson, V., Schanen, D., Meyer, N., & Craig, C. (2012). Unified parameterization of the planetary boundary layer and shallow convection with a higher-order turbulence closure in the Community Atmosphere Model: Single-column experiments. *Geoscientific Model Development*, 5(6), 1407–1423. <https://doi.org/10.5194/gmd-5-1407-2012>
- Bogenschutz, P. A., Yamaguchi, T., & Lee, H. H. (2021). The Energy Exascale Earth System Model simulations with high vertical resolution in the lower troposphere. *Journal of Advances in Modeling Earth Systems*, 13(6), e2020MS002239. <https://doi.org/10.1029/2020MS002239>
- Fielding, M. D., Schäfer, S. A., Hogan, R. J., & Forbes, R. M. (2020). Parametrizing cloud geometry and its application in a subgrid cloud-edge erosion scheme. *Quarterly Journal of the Royal Meteorological Society*, 146(729), 1651–1667. <https://doi.org/10.1002/qj.3758>
- Golaz, J. C., Caldwell, P. M., Van Roekel, L. P., Petersen, M. R., Tang, Q., Wolfe, J. D., et al. (2019). The DOE E3SM coupled model version 1: Overview and evaluation at standard resolution. *Journal of Advances in Modeling Earth Systems*, 11(7), 2089–2129. <https://doi.org/10.1029/2018MS001603>
- Golaz, J.-C., Larson, V. E., & Cotton, W. R. (2002). A PDF-based model for boundary layer clouds. Part I: Method and model description. *Journal of the Atmospheric Sciences*, 59(24), 3540–3551. [https://doi.org/10.1175/1520-0469\(2002\)059<3540:APBMFB>2.0.CO;2](https://doi.org/10.1175/1520-0469(2002)059<3540:APBMFB>2.0.CO;2)
- Grabowski, W. W. (2001). Coupling cloud processes with the large-scale dynamics using the cloud-resolving convection parameterization (CRCP). *Journal of the Atmospheric Sciences*, 58(9), 978–997. [https://doi.org/10.1175/1520-0469\(2001\)058<0978:CCPWTL>2.0.CO;2](https://doi.org/10.1175/1520-0469(2001)058<0978:CCPWTL>2.0.CO;2)
- Gu, Y., & Liou, K. (2001). Radiation parameterization for three-dimensional inhomogeneous cirrus clouds: Application to climate models. *Journal of Climate*, 14(11), 2443–2457. [https://doi.org/10.1175/1520-0442\(2001\)014<2443:rpfidi>2.0.co;2](https://doi.org/10.1175/1520-0442(2001)014<2443:rpfidi>2.0.co;2)
- Hersbach, H., Bell, B., Berrisford, P., Biavati, G., Horányi, A., Muñoz Sabater, J., et al. (2023). ERA5 monthly averaged data on pressure levels from 1940 to present [Dataset]. *Copernicus Climate Change Service (C3S) Climate Data Store (CDS)*. <https://doi.org/10.24381/cds.6860a573>
- Hogan, R. J. (2020). ECMWF atmospheric radiation scheme (Version 1.4.0) [Software]. GitHub. Retrieved from <https://github.com/ecmwf/ecrad>
- Hogan, R. J., & Bozzo, A. (2018). A flexible and efficient radiation scheme for the ECMWF model. *Journal of Advances in Modeling Earth Systems*, 10(8), 1990–2008. <https://doi.org/10.1029/2018MS001364>
- Hogan, R. J., Fielding, M. D., Barker, H. W., Villefranque, N., & Schäfer, S. A. (2019). Entrapment: An important mechanism to explain the shortwave 3D radiative effect of clouds. *Journal of the Atmospheric Sciences*, 76(7), 2123–2141. <https://doi.org/10.1175/JAS-D-18-0366.1>
- Hogan, R. J., & Illingworth, A. J. (2000). Deriving cloud overlap statistics from radar. *Quarterly Journal of the Royal Meteorological Society*, 126(569), 2903–2909. <https://doi.org/10.1002/qj.49712656914>
- Hogan, R. J., Schäfer, S. A., Klinger, C., Chiu, J. C., & Mayer, B. (2016). Representing 3-D cloud radiation effects in two-stream schemes: 2. Matrix formulation and broadband evaluation. *Journal of Geophysical Research: Atmospheres*, 121(14), 8583–8599. <https://doi.org/10.1002/2016JD024875>
- Hogan, R. J., & Shonk, J. K. (2013). Incorporating the effects of 3D radiative transfer in the presence of clouds into two-stream multilayer radiation schemes. *Journal of the Atmospheric Sciences*, 70(2), 708–724. <https://doi.org/10.1175/JAS-D-12-041.1>
- Jakub, F., & Mayer, B. (2015). A three-dimensional parallel radiative transfer model for atmospheric heating rates for use in cloud resolving models—The TenStream solver. *Journal of Quantitative Spectroscopy and Radiative Transfer*, 163, 63–71. <https://doi.org/10.1016/j.jqsrt.2015.05.003>
- Jakub, F., & Mayer, B. (2017). The role of 1-D and 3-D radiative heating in the organization of shallow cumulus convection and the formation of cloud streets. *Atmospheric Chemistry and Physics*, 17(21), 13317–13327. <https://doi.org/10.5194/acp-17-13317-2017>
- Jing, X., Zhang, H., Peng, J., Li, J., & Barker, H. W. (2016). Cloud overlapping parameter obtained from CloudSat/CALIPSO dataset and its application in AGCM with McICA scheme. *Atmospheric Research*, 170, 52–65. <https://doi.org/10.1016/j.atmosres.2015.11.007>
- Jing, X., Zhang, H., Satoh, M., & Zhao, S. (2018). Improving representation of tropical cloud overlap in GCMs based on cloud-resolving model data. *Journal of Meteorological Research*, 32(2), 233–245. <https://doi.org/10.1007/s13351-018-7095-9>
- Kablick, G. P., Ellingson, R. G., Takara, E. E., & Gu, J. (2011). Longwave 3D benchmarks for inhomogeneous clouds and comparisons with approximate methods. *Journal of Climate*, 24(8), 2192–2205. <https://doi.org/10.1175/2010JCLI3752.1>

- Khairoutdinov, M. F., & Randall, D. A. (2001). A cloud resolving model as a cloud parameterization in the NCAR Community Climate System Model: Preliminary results. *Geophysical Research Letters*, 28(18), 3617–3620. <https://doi.org/10.1029/2001GL013552>
- Klinger, C., Feingold, G., & Yamaguchi, T. (2019). Cloud droplet growth in shallow cumulus clouds considering 1-D and 3-D thermal radiative effects. *Atmospheric Chemistry and Physics*, 19(9), 6295–6313. <https://doi.org/10.5194/acp-19-6295-2019>
- Klinger, C., Mayer, B., Jakub, F., Zinner, T., Park, S.-B., & Gentine, P. (2017). Effects of 3-D thermal radiation on the development of a shallow cumulus cloud field. *Atmospheric Chemistry and Physics*, 17(8), 5477–5500. <https://doi.org/10.5194/acp-17-5477-2017>
- Lebrun, R., Dufresne, J. L., & Villefranque, N. (2023). A consistent representation of cloud overlap and cloud subgrid vertical heterogeneity. *Journal of Advances in Modeling Earth Systems*, 15(6), e2022MS003592. <https://doi.org/10.1029/2022MS003592>
- Lee, H. H., Bogenschütz, P., & Yamaguchi, T. (2021). The implementation of framework for improvement by vertical enhancement into Energy Exascale Earth System Model. *Journal of Advances in Modeling Earth Systems*, 13(6), e2020MS002240. <https://doi.org/10.1029/2020MS002240>
- Lilly, D. K. (1968). Models of cloud-topped mixed layers under a strong inversion. *Quarterly Journal of the Royal Meteorological Society*, 94(401), 292–309. <https://doi.org/10.1002/qj.49709440106>
- Marshak, A., Platnick, S., Várnai, T., Wen, G., & Cahalan, R. F. (2006). Impact of three-dimensional radiative effects on satellite retrievals of cloud droplet sizes. *Journal of Geophysical Research*, 111(D9), D09207. <https://doi.org/10.1029/2005JD006686>
- Meador, W., & Weaver, W. (1980). Two-stream approximations to radiative transfer in planetary atmospheres: A unified description of existing methods and a new improvement. *Journal of the Atmospheric Sciences*, 37(3), 630–643. [https://doi.org/10.1175/1520-0469\(1980\)037<0630:TSATRT>2.0.CO;2](https://doi.org/10.1175/1520-0469(1980)037<0630:TSATRT>2.0.CO;2)
- Mlawer, E. J., Taubman, S. J., Brown, P. D., Iacono, M. J., & Clough, S. A. (1997). Radiative transfer for inhomogeneous atmospheres: RRTM, a validated correlated-k model for the longwave. *Journal of Geophysical Research*, 102(D14), 16663–16682. <https://doi.org/10.1029/97JD00237>
- Pincus, R., Barker, H. W., & Morcrette, J. J. (2003). A fast, flexible, approximate technique for computing radiative transfer in inhomogeneous cloud fields. *Journal of Geophysical Research*, 108(D13), 4376. <https://doi.org/10.1029/2002JD003322>
- Platnick, S., Meyer, K. G., King, M. D., Wind, G., Amarasinghe, N., Marchant, B., et al. (2017). The MODIS cloud optical and microphysical products: Collection 6 updates and examples from Terra and Aqua. *IEEE Transactions on Geoscience and Remote Sensing*, 55(1), 502–525. <https://doi.org/10.1109/TGRS.2016.2610522>
- Pressel, K. G., Kaul, C. M., Schneider, T., Tan, Z., & Mishra, S. (2015). Large-eddy simulation in an anelastic framework with closed water and entropy balances. *Journal of Advances in Modeling Earth Systems*, 7(3), 1425–1456. <https://doi.org/10.1002/2015MS000496>
- Ren, T. (2023). Caltech LES 3D cloud fields and associated forcing data (Version 1) [Dataset]. Texas Data Repository. <https://doi.org/10.18738/T8/T9RQMP>
- Ren, T., Yang, P., Schumacher, C., Huang, X., & Lin, W. (2020). Impact of cloud longwave scattering on radiative fluxes associated with the Madden-Julian Oscillation in the Indian Ocean and Maritime Continent. *Journal of Geophysical Research: Atmospheres*, 125(13), e2020JD032591. <https://doi.org/10.1029/2020JD032591>
- Ren, T., Yang, P., Wei, J., Huang, X., & Sang, H. (2022). Performance of cloud 3D solvers in ice cloud shortwave radiation closure over the equatorial western Pacific Ocean. *Journal of Advances in Modeling Earth Systems*, 14(2), e2021MS002754. <https://doi.org/10.1029/2021MS002754>
- Schäfer, S. A., Hogan, R. J., Klinger, C., Chiu, J. C., & Mayer, B. (2016). Representing 3-D cloud radiation effects in two-stream schemes: 1. Longwave considerations and effective cloud edge length. *Journal of Geophysical Research: Atmospheres*, 121(14), 8567–8582. <https://doi.org/10.1002/2016JD024876>
- Shen, Z., Pressel, K. G., Tan, Z., & Schneider, T. (2020). Statistically steady state large-eddy simulations forced by an idealized GCM: 1. Forcing framework and simulation characteristics. *Journal of Advances in Modeling Earth Systems*, 12(2), e2019MS001814. <https://doi.org/10.1029/2019MS001814>
- Shen, Z., Sridhar, A., Tan, Z., Jaruga, A., & Schneider, T. (2022). A library of large-eddy simulations forced by global climate models. *Journal of Advances in Modeling Earth Systems*, 14(3), e2021MS002631. <https://doi.org/10.1029/2021MS002631>
- Shonk, J. K., & Hogan, R. J. (2008). Tripleclouds: An efficient method for representing horizontal cloud inhomogeneity in 1D radiation schemes by using three regions at each height. *Journal of Climate*, 21(11), 2352–2370. <https://doi.org/10.1175/2007JCL1940.1>
- Singer, C. E., Lopez-Gomez, I., Zhang, X., & Schneider, T. (2021). Top-of-atmosphere albedo bias from neglecting three-dimensional cloud radiative effects. *Journal of the Atmospheric Sciences*, 78(12), 4053–4069. <https://doi.org/10.1175/JAS-D-21-0032.1>
- Stamnes, K., Tsay, S.-C., Wiscombe, W., & Jayaweera, K. (1988). Numerically stable algorithm for discrete-ordinate-method radiative transfer in multiple scattering and emitting layered media. *Applied Optics*, 27(12), 2502–2509. <https://doi.org/10.1364/AO.27.002502>
- Taylor, K. E., Stouffer, R. J., & Meehl, G. A. (2012). An overview of CMIP5 and the experiment design. *Bulletin of the American Meteorological Society*, 93(4), 485–498. <https://doi.org/10.1175/BAMS-D-11-00094.1>
- Veerman, M., Pedruzo-Bagazgoitia, X., Jakub, F., Vilà-Guerau de Arellano, J., & van Heerwaarden, C. (2020). Three-dimensional radiative effects by shallow cumulus clouds on dynamic heterogeneities over a vegetated surface. *Journal of Advances in Modeling Earth Systems*, 12(7), e2019MS001990. <https://doi.org/10.1029/2019MS001990>
- Veerman, M., van Stratum, B., & van Heerwaarden, C. (2022). A case study of cumulus convection over land in cloud-resolving simulations with a coupled ray tracer. *Geophysical Research Letters*, 49(23), e2022GL100808. <https://doi.org/10.1029/2022GL100808>
- Villefranque, N., Blanco, S., Couvreux, F., Fournier, R., Gautrais, J., Hogan, R. J., et al. (2021). Process-based climate model development harnessing machine learning: III. The representation of cumulus geometry and their 3D radiative effects. *Journal of Advances in Modeling Earth Systems*, 13(4), e2020MS002423. <https://doi.org/10.1029/2020MS002423>
- Villefranque, N., & Hogan, R. J. (2021). Evidence for the 3D radiative effects of boundary-layer clouds from observations of direct and diffuse surface solar fluxes. *Geophysical Research Letters*, 48(14), e2021GL093369. <https://doi.org/10.1029/2021GL093369>
- Wyant, M. C., Bretherton, C. S., Rand, H. A., & Stevens, D. E. (1997). Numerical simulations and a conceptual model of the stratocumulus to trade cumulus transition. *Journal of the Atmospheric Sciences*, 54(1), 168–192. [https://doi.org/10.1175/1520-0469\(1997\)054<0168:NSAACM>2.0.CO;2](https://doi.org/10.1175/1520-0469(1997)054<0168:NSAACM>2.0.CO;2)
- Yamaguchi, T., Feingold, G., & Larson, V. E. (2017). Framework for improvement by vertical enhancement: A simple approach to improve representation of low and high-level clouds in large-scale models. *Journal of Advances in Modeling Earth Systems*, 9(1), 627–646. <https://doi.org/10.1002/2016MS000815>